HHS Public Access

Author manuscript

Neuron. Author manuscript; available in PMC 2016 October 21.

Published in final edited form as:

Neuron. 2015 October 21; 88(2): 390–402. doi:10.1016/j.neuron.2015.09.033.

Orientation selectivity sharpens motion detection in Drosophila

Yvette E. Fisher[*,1], **Marion Silies**[*,1,2], and **Thomas R. Clandinin**[1]

[1]Dept. of Neurobiology, Stanford University, Stanford, CA, 94305, USA

SUMMARY

Detecting the orientation and movement of edges in a scene is critical to visually guided behaviors of many animals. What are the circuit algorithms that allow the brain to extract such behaviorally vital visual cues? Using *in vivo* two-photon calcium imaging in *Drosophila*, we describe direction selective signals in the dendrites of T4 and T5 neurons, detectors of local motion. We demonstrate that this circuit performs selective amplification of local light inputs, an observation that constrains motion detection models and confirms a core prediction of the Hassenstein-Reichardt Correlator (HRC). These neurons are also orientation selective, responding strongly to static features that are orthogonal to their preferred axis of motion, a tuning property not predicted by the HRC. This coincident extraction of orientation and direction sharpens directional tuning through surround inhibition and reveals a striking parallel between visual processing in flies and vertebrate cortex, suggesting a universal strategy for motion processing.

INTRODUCTION

Visual scenes contain differences in brightness, creating contrasts that define edges with particular orientations in space. Detecting the motion of these edges guides a diverse array of adaptive behaviors in many animals (Gibson, 1950). Neurons that are tuned to detect either motion or orientation, or both, have been described in many systems, including insects, fish, mice, and primates (Borst, 2014; DeAngelis et al., 1995; Niell and Smith, 2005; Niell and Stryker, 2008). Thus, understanding the circuit algorithms that underlie the extraction of motion and orientation cues is a broad challenge, and it is unclear whether the simultaneous encoding of these features represents a universal processing strategy. Here, we take advantage of a powerful genetic system, the fruit fly *Drosophila melanogaster*, to define the relationship between direction selectivity and orientation preference within motion detecting circuits.

Correspondence: trc@stanford.edu.

[2]Present address: European Neuroscience Institute, Grisebachstr. 5, 37077, Göttingen, Germany

[*]These authors contributed equally to this work

AUTHOR CONTRIBUTIONS

YEF, MS and TRC designed the study, YEF and MS performed the experiments and analyzed the data, and YEF, MS and TRC wrote the manuscript.

Motion detecting circuits compare signals across space and time. Circuits that respond selectively to motion in a particular direction across a restricted region of visual space are termed elementary motion detectors. Three classes of theoretical models, the Hassenstein-Reichardt Correlator (HRC, Hassenstein & Reichardt 1956), the Barlow and Levick model (B-L; Barlow and Levick, 1965), and the motion energy model (Adelson & Bergen 1985) have been proposed to implement elementary motion detection. All of these models process input signals along one axis of space. Along this axis, they respond more strongly to motion in a preferred direction (PD) than to motion in the opposite, or null direction (ND). However, they differ in the computational operations that produce this selectivity.

In vertebrate primary visual cortex, neurons that display direction selectivity invariably also display orientation selectivity, the preference for edges with a particular orientation in space (DeAngelis et al., 1995). Thus, early studies proposed that combining direction selectivity with orthogonal orientation selectivity plays an important part in the perception of motion (Hubel and Wiesel, 1959). In this context, the stimulus that would create the strongest motion signal would be an edge oriented orthogonal to the axis of direction preference (Henry et al., 1974). However, the relationship between orientation selective (OS) and direction selective (DS) tuning properties has not been extensively investigated for elementary motion detectors in the fly visual system. Thus it is unclear whether simultaneous extraction of both of these two higher order features, orientation and motion direction, is fundamental to motion processing.

Fruit flies have long provided a powerful context in which to study motion processing, and neural substrates of local motion detection have recently been proposed (Behnia et al., 2014; Maisak et al., 2013). However, it is unknown how elementary motion detection is implemented, nor is it clear how the computation is performed at the cellular level. In the *Drosophila* visual system, motion detection is performed within distinct circuits specialized for either moving light (ON) or dark (OFF) edges. Visual information is relayed from photoreceptors onto interneurons within a retinotopically organized neuropil called the lamina. Electrophysiological and behavioral studies have shown that the first order interneurons L1, L2 and L3 provide input to distinct motion pathways. The detection of moving light edges requires input from L1, while circuits that detect moving dark edges receive strong inputs from L2 and L3 (Clark et al., 2011; Joesch et al., 2010; Silies et al., 2013). Recent anatomical and physiological studies have described columnar neurons that link the lamina neurons with T4 and T5 and have spatial offsets and temporal delays relevant to motion detection (Behnia et al., 2014; Meier et al., 2014; Shinomiya et al., 2014; Takemura et al., 2013). It has been proposed that direction selectivity for moving ON and OFF edges arises in T4 and T5 respectively, by an interaction between these delayed and non-delayed columnar neurons (Behnia et al., 2014; Maisak et al., 2013; Ammer et al., 2015). Nonetheless, the specific computation that links these non-directional inputs to DS outputs in T4 and T5 is unknown (Borst, 2014). Here we use *in vivo* two-photon calcium imaging in T4 and T5 to define this computation.

RESULTS

T4 and T5 dendrites are directionally tuned

To capture signals about motion in all directions, there are four subtypes of both T4 and T5, each of which is tuned to motion in one of the four cardinal directions (Maisak et al., 2013). These cell types are arranged retinotopically such that each individual neuron only responds to a particular direction of motion at a specific location in visual space. T4 and T5 dendrites innervate distinct layers in two regions of the visual system, the medulla and lobula, respectively, while the axons of both cell types project to a third region, the lobula plate (Fischbach and Dittrich, 1989). Within the lobula plate, axons from the subtypes of T4 and T5 that respond selectively to the same direction of motion innervate the same layer, creating a layer-specific pattern of directional preferences (Figure 1A; Maisak et al. 2013; Buchner et al. 1984). One model that has been proposed is that these directional responses arise within the dendrites of T4 and T5, where non-DS synaptic inputs could interact post-synaptically to compute motion direction (Borst 2014). However, within both the medulla and the lobula, dendrites from cells with different directional preferences are spatially intermingled, making direct visualization of single cell responses challenging. As a result, DS responses of these cells have only been observed in fibers of passage and axon terminals, not dendrites (Maisak et al., 2013). In particular, DS responses to moving gratings were observed within fibers of passage labeled by a driver line that marks both T4 and T5, suggesting that DS may arise prior to the axon terminal in some of these cells (Maisak et al. 2013). However, it remains an open question whether the dendrites of individual T4 and T5 neurons are DS, an important constraint on the biological implementation of motion detection.

To directly determine whether DS signals in T4 and T5 first emerge in their dendrites, we took genetic approaches that allowed us to measure the responses from dendrites of single subtypes of T4 and T5 (Figure 1). We expressed the calcium indicator GCaMP6f in T4 and T5 under the control of different genetic drivers, and used *in vivo* two-photon calcium imaging to measure changes in intracellular calcium levels during the presentation of motion stimuli (Figure S1). To measure DS responses, a single bar or edge moving in different directions was displayed to the animal (Figure S1A). As expected, responses from axon terminals within a single layer of the lobula plate displayed robust direction selectivity (Figure S1B). To separate the responses of T4 and T5 axons, we used single moving ON and OFF edge stimuli. As predicted, when calcium signals were monitored in both T4 and T5, DS responses to both edge types were observed within the same layer, likely representing the distinct responses of T4 and T5 to each edge (Figure 1A; Maisak et al. 2013).

To investigate the DS tuning properties of the dendrites of T4, we identified a T4-GAL4 driver line that almost exclusively expressed GCaMP6f within a single subtype (Figure 1B, Figure S1C, D). Using this driver line, we observed that T4 dendrites displayed DS responses to moving ON edges, but did not respond to moving OFF edges (Figure 1B). Quantitatively, the magnitude of direction selectivity measured in a large population of T4 dendrites was only slightly weaker than that of their cognate terminals (Figure 1E, Figure S1F). Thus, strong direction selectivity exists at the level of T4 dendrites.

Next, we tested if the dendrites of T5 were also DS. As expected from the intermingling of the four subtypes, T5 dendrites imaged using the T4/T5 driver line responded specifically to OFF edges but responded strongly to motion in all directions (Figure 1 C, F). Since we did not have a driver line that expressed in only one T5 subtype, we adapted a stochastic labeling approach to isolate the responses of single dendrites (Gordon and Scott, 2009; Gruntman and Turner, 2013). We used a Flippase-based mosaic method to label a subset of T4 and T5 neurons (Figure 1D, Figure S1E). Imaging of stochastically labeled T5 dendrites revealed a wide range of DS responses (Figure 1F, G). However, we observed many isolated T5 dendrites that displayed strong direction selectivity for moving dark edges, consistent with these dendrites representing the processes of single cells (24 regions of interest (ROIs) with a DS index of > 0.5, Figure 1D, F, G). As a population, sparsely labeled T5 dendrites displayed increased directional tuning when compared to dendrites imaged in the driver line that labels all subtypes (Figure S1G). The most strongly tuned T5 dendrites were as tuned as T5 axon terminals (Figure 1G). Given that the major synaptic inputs to T4 and T5 are not directionally tuned (Behnia et al., 2014), these data argue strongly that direction selectivity emerges in the dendrites of T4 and T5.

T4 and T5 amplify preferred direction signals

What is the structure of the computation that extracts these elementary motion signals? HRC and motion energy models make distinct predictions about how DS tuning is achieved relative to B-L models. In HRC and motion energy models signals moving in the PD are selectively enhanced, while in B-L models, inputs moving in the non-preferred direction are specifically suppressed. A classical test to distinguish between these models makes use of apparent motion stimuli in which two spatially distinct static stimuli are presented sequentially with varying temporal delays (Figure 2), (Egelhaaf and Borst, 1992; Hassenstein and Reichardt, 1956). We presented a single 3° wide bar that extended the full length of the screen that was either darker or lighter than the background at a single point in space and then, at a variable later time, presented a pair of bars, with one at the original location and one shifted by 2° (Figure 2A). This spatial offset was chosen to approximately activate adjacent facets of the retina. By presenting this sequence of bars we generated apparent motion stimuli that represented either moving light edges, or moving dark edges, allowing us to isolate responses from the ON or OFF pathway. If the time delay between the two stimulation periods is brief, this stimulus appears as motion in the direction of the second bar. With long temporal delays, the stimulus no longer appears as motion, and the circuit responds independently to each stimulus element. These individual responses can be used to build a linear prediction for how neurons would respond to the combination of these inputs if the signals at the short delays relevant to motion detection were handled identically to signals at longer time scales (Figure 2B, C). In this manner, symmetric PD and ND stimuli can be compared with their linear predictions (Figure 2B, C). All models of motion detection predict that responses to these stimuli with short delays will be larger in the PD than in the ND. However, how this difference is achieved varies between the models. HRC models predict a supralinear response to the PD, relative to a linear ND response (Figure 2B), while B-L models predict a sublinear response to the ND and a linear response to the PD (Figure 2C).

Using a set of these stimuli with either dark or light bars, we observed DS responses in the lobula plate across a range of time delays, with differences between PD and ND responses observed for delays between 8 ms and 500 ms, depending on the stimulus (Figure 2D,E,G, Figure 3A,B,D, Figure S2A and data not shown). These delays closely match delays that evoked DS responses measured in lobula plate tangential cells in blowflies using analogous stimuli (Egelhaaf and Borst, 1992). As expected, different layers displayed distinct apparent motion preferences that matched their DS responses to real motion, with T4 and T5 responding to light and dark stimuli, respectively (Figure 2D, E, G, Figure 3A, B, D; Figure S2 and data not shown).

To assess the underlying circuit computation performed by the ON pathway we compared the measured responses to the bright bar apparent motion stimuli with predictions based on a linear interaction, as described above. Importantly, at brief delays, PD responses to these apparent motion stimuli were significantly larger than the linear prediction, consistent with non-linear amplification (Figure 2D,H). Conversely, ND responses were typically linear, with only a weakly sub-linear response observed specifically at the 50ms delay (Figure 2E,I).

Since these apparent motion stimuli sequentially activate the same location in space both before and after the temporal delay, we reasoned that circuit mechanisms independent of motion, such as light adaptation or sensitization, might also be engaged. To test whether this pathway might exhibit such facilitation or depression in response to these sequential light inputs we utilized two different “flash-control” stimuli that preserve the same temporal structure without generating a motion signal. In the first stimulus, a pair of bars was presented twice at the same location using the same temporal delays as the apparent motion stimuli. Using this control we observed approximately linear responses (Figure 2F,J, Figure S2C). The second flash control stimulus presented a single bar twice at one of the two adjacent locations used to produce apparent motion. Again, the responses to single bar flashes were linear for all temporal intervals tested, at both spatial positions (Figure S2F, Figure S3). Together, these control experiments demonstrate that the ON pathway does not display either facilitation or depression in response to these sequential light inputs. Thus, selective amplification of PD motion is a critical local interaction that establishes direction selectivity in these neurons.

Does the OFF pathway employ a similar circuit algorithm? As we observed for bright bars, in response to apparent motion stimuli comprising dark bars, PD responses were dramatically larger than the corresponding linear predictions, again consistent with a non-linear interaction between inputs (Figure 3A,E). Interestingly, however, we also observed sub-linear responses to ND stimuli using dark bars, across the same range of delays that showed non-linear amplification of the PD signals (Figure 3B,F). This divergence from linearity for both PD and ND signals could reflect the possibility that the OFF pathway exploits both amplifying and suppressive mechanisms, or it could be due to circuit processing effects that are independent of motion. To quantify these latter effects, we utilized dark bar “flash-control” stimuli. Surprisingly, unlike the ON pathway, we observed responses that were significantly smaller than the linear prediction using the “flash” control stimulus that contained a pair of dark bars (Figure 3G). This sub-linear effect was of similar

magnitude and arose across the same temporal delays as the suppression observed for ND responses to the apparent motion stimuli (Figure 3F,G). Thus, for T5, the ND suppression observed using dark bar apparent motion stimuli is unlikely to be produced by the motion computation *per se*, but rather is most likely to reflect circuit adaptation to sequential inputs. Importantly, responses to the flash control stimuli in which single bars were presented at each point in space were small in magnitude and typically linear (Figure S3A), ruling out the possibility that a spatially local facilitating interaction contributes to the amplification we observed using the apparent motion stimuli.

Taken together, these data demonstrate that the dominant interaction that produces DS responses to local signals in both T4 and T5 is a selective non-linear amplification of PD inputs, as predicted by the HRC and motion energy models. We note that the magnitude of the PD enhancement we observed in T5 is likely an underestimate of the true amplification seen in the circuit, once the adaptation effects we observed using flash control stimuli are accounted for. Thus, we propose that local DS responses emerge in T4 and T5 dendrites through coincident detection of adjacent input signals that are combined in a supra-linear manner.

T4 and T5 are tightly orientation selective

Having characterized the motion computation performed within the receptive field center of T4 and T5, we wondered how other spatial receptive field properties might shape T4 and T5 responses. In primary visual cortex, DS neurons are almost invariably also OS, having a sharp preference for a particular orientation of an edge in space (DeAngelis et al., 1995). Conversely, DS ganglion cells in the vertebrate retina do not display consistent orientation tuning. We next explored whether this DS circuit in the fly was orientation tuned. To do this, we presented static square wave gratings at 12 different orientations, and recorded the responses of T4 and T5 terminals (Figure 4A). Strikingly, all four layers of the lobula plate displayed strong orientation tuning, with axon terminals in layers A and B displaying preferential responses to features that were approximately vertically oriented, while terminals in layers C and D were tuned to respond to horizontal features. These results are consistent with previous observations in which the responses of T4 and T5 cells to counterphase flicker depended on the orientation of the stimulus (Maisak et al., 2013). Thus, in addition to direction selectivity, T4 and T5 are also tuned to respond to static features with particular orientations.

What are the circuit mechanisms that lead to these OS responses? In vertebrate cortex, orientation selectivity emerges from combinations of excitatory and inhibitory subregions within the spatial receptive field. Interestingly, recent work has demonstrated that several of the critical inputs to T5, including the lamina neuron L2 and the medulla interneurons Tm1 and Tm2, have antagonistic center-surround receptive fields meaning that light inputs from different spatial locations have distinct effects on the outputs of these cells (Freifeld et al., 2013; Meier et al., 2014; Strother et al., 2014). We therefore sought to determine if the receptive fields of T4 and T5 had an antagonistic center-surround structure.

We first determined the spatial positions of the receptive fields for each population of T4 and T5 axon terminals using moving bar stimuli (Freifeld et al., 2013). Next, we presented

static vertical and horizontal dark and light bars of varying width, centered on the responsive location (Figure 4B, C and Figure S4). As expected from our experiments using gratings, different layers displayed clear preferences for particular bar orientations, favoring either horizontal or vertical bars. For the preferred bar orientation, response was dependent on bar width. For example, in layers C and D, 2° wide dark bars elicited weak responses from T5 axons, but wider bars evoked progressively stronger responses for bar widths of up to 15°. As bar width was further increased, responses grew weaker, demonstrating that these cells have an antagonistic center-surround organization (Figure 4C). For layers A and B, we observed responses for vertical dark bar widths of between 5° and 30° (Figure 4B). The relatively modest response amplitudes recorded from layer A and B likely reflect the fact that it was more difficult to obtain aligned single bar responses from these neurons because of their retinotopic organization relative to the imaging plane. Nonetheless, in all cases, we observe an antagonistic surround that was sufficiently strong to completely abrogate all responses to full screen illumination (covering approximately 50° of visual angle; Figure 4B, C). To stimulate T4 cells, we used bright bars on a dark background. As above, we observed larger responses to narrower bars than to wide bars, again consistent with an antagonist center-surround receptive field (Figure S4). Thus, both T4 and T5 have antagonistic center-surround receptive fields. Finally, we used the responses to bars of intermediate size that drove strong responses to compare orientation selectivity between T4 and T5. Orientation selectivity of each layer was consistent for both dark and light bars, demonstrating that in addition to displaying matching laminar organization for DS, the ON and OFF pathways appeared to have matched OS (Figure 4 D , E).

Individual T4 and T5 neurons display orientation selectivity

Given that the axon terminals of T4 and T5 are arrayed retinotopically, we reasoned that ROIs selected from the lobula plate might contain more than one neighboring axon terminal, meaning that OS could arise by mixing signals from cells which individually do not display a strong orientation preference. To probe the responses of individual T4 and T5 neurons we again sparsely labeled neurons using the mosaic method (Figure 1) and imaged axon terminals in the lobula plate. We observed many individual regions of interest that were selective for a single moving edge type and that displayed strong direction selectivity consistent with single T4 or T5 clones (Figure S4D,E,F,G). Putative single axon terminals were selected for the analysis only if they displayed strong direction tuning for either moving ON or OFF edges (DSI >0.5; Figure S4E,G). Importantly, many of these individual terminals were strongly OS in response to the presentation of static square-wave gratings at different orientations (Figure 4F,H). The orientation tuning of these individual clones was not significantly different than the distribution of orientation tuning measured from ROIs drawn from the dense labeling seen in the T4/T5 driver line (Figure 4G,I, Figure S4H). Thus, individual T4 and T5 axon terminals display prominent orientation tuning, indicating that orientation selectivity is not an emergent phenomenon that arises from mixing of neuronal signals.

Inhibitory circuitry is required for orientation and direction selectivity

We hypothesized that inhibitory circuits could account for both OS and center- surround antagonism (Figure S5). Since T4 and T5 signals are shaped by many upstream neurons with

antagonistic center-surround receptive fields (Freifeld et al., 2013; Meier et al., 2014; Strother et al., 2014), we reasoned that a pharmacological approach would be necessary to determine the overall contribution of inhibitory circuits to T4 and T5 response properties.

To test whether inhibitory circuits are required for the orientation selectivity and spatial surround of T4 and T5, we imaged axon terminals and applied the chloride channel antagonist picrotoxin. Remarkably, application of picrotoxin abolished OS responses to static gratings across all four layers (Figure 5A). This loss of orientation tuning was not reflective of response saturation due to disinhibition, as responses to gratings with lower contrasts that were much smaller in amplitude were similarly affected(Figure S5A). In addition, application of picrotoxin disrupted spatial surround antagonism for both dark and light bars (Figure 5B,C, Figure S5B,C). The response magnitude for dark bars but not light bars was greatly increased compared to controls (Figure 5B,C, Figure S5 B, C). We further used these single bar stimuli to separate the effects of picrotoxin on T4 and T5 orientation selectivity. With light bars, OS responses were lost across all layers in the lobula plate (Figure 5E). Using dark bars, OS responses were completely lost in layers A and B, and significantly degraded in layers C and D, with these layers retaining a preference for horizontal bars (Figure 5D). This remaining OS may reflect incomplete drug activity. Taken together, these data reveal that inhibitory signaling plays a vital role in shaping the antagonistic surround and in conferring orientation selectivity to T4 and T5.

Given such a profound effect of inhibition on T4 and T5 spatial receptive fields, we reasoned that inhibitory circuits might also contribute to direction selectivity. Upon application of picrotoxin, the responses of T4 and T5 axon terminals to a moving dark bar lost directional tuning (Figure 6A). In particular, PD responses remained the same size while responses to bars moving in the ND increased in magnitude, becoming as large as the PD responses (Figure 6A).

One possible interpretation of these data is that picrotoxin indiscriminately disinhibits T4 and T5 such that motion in any direction would produce a saturating response. To test this possibility, we varied the strength of the directional stimulus by lowering the contrast of the moving bar. Under these conditions, picrotoxin application reduced direction selectivity similarly across all tested contrasts, even when responses were greatly reduced in magnitude relative to those observed using high contrast stimuli (Figure 6B).

In flies, picrotoxin blocks both GABA-A receptors and inhibitory glutamate-gated chloride channels, albeit at different concentrations (Ffrench-Constant et al., 1993; Liu and Wilson, 2013; Mauss et al., 2014). To test the specific contribution of GABA-A receptors to the effects of picrotoxin on this circuit, we used a mutation in the GABA-A receptor gene *Resistance to Dieldrin* (Rdl) that is insensitive to picrotoxin, but can still respond normally to GABA (Ffrench-Constant et al., 1993). In this mutant background, the normal DS responses of T4 and T5 were largely unaffected by the addition of the drug (Figure S6A–D). Similarly, in this mutant background, picrotoxin also had no effect on the antagonistic spatial surround, as measured by full field illumination (Figure S6E). Thus, much of picrotoxin's effect on response properties reflect blockade of GABA-A receptors.

To test whether blocking inhibitory circuits equally affected both cell types, we recorded calcium signals within T4 or T5 dendrites before and after picrotoxin application, while displaying a stimulus that had moving light and dark edges. Upon drug application, T4 dendrites of a single subtype displayed a small reduction in direction selectivity (Figure S6F). However, in stochastically labeled and strongly DS T5 dendrites, picrotoxin application abolished directional tuning (Figure S6G). Thus, blocking inhibitory circuitry affects the directional tuning of both T4 and T5, with more prominent effects on T5. Finally, we note that picrotoxin application also disrupted directional tuning to apparent motion stimuli in both cells (Figure S6H, I). This effect may be accounted for by the fact that picrotoxin application substantially shortens response latencies to static stimuli (data not shown), suggesting that in addition to shaping center-surround receptive fields, inhibitory signaling also shapes signals in time within the motion pathways. Taken together our data demonstrate that both the orientation selectivity and direction preference of T4 and T5 require inhibitory circuitry.

An orthogonal interaction between OS and DS can sharpen DS tuning

Our observations mapping orientation selectivity using static gratings (Figure 4) were consistent with the notion that the axis of orientation preference was approximately orthogonal to the axis of direction selectivity. To test this idea directly, we presented static gratings that then moved in one of twelve directions, allowing us to map orientation selectivity to static stimuli as well as direction selectivity to moving stimuli for the same axon terminals (Figure 7A). Using this stimulus we observed, for example, that axon terminals in lobula plate layer A responded strongly both to gratings moving in the PD as well as to the presentation of static gratings oriented orthogonal to the axis of motion preference (Figure 7B). When the same axon terminals were presented with a static grating that then moved in the ND, we observed an initial response to the static cue, followed by a plateau during the motion epoch (Figure 7C). Gratings of other directions produced responses that were often even smaller than responses observed for the ND (Figure 7D). From these population responses, we constructed plots of orientation and direction tuning (Figure 7E). Comparing the angles of preferred orientation and direction vectors for each axon terminal revealed that the offset between these two angles tightly clustered around 90° (Figure 7F). Thus, orientation and direction selectivity are orthogonal in T4 and T5.

Does the oriented receptive field of T4 and T5, which is systematically orthogonal to the axis of direction selectivity, impact motion detection? In the standard HRC model, a “half-correlator” samples along a single spatial dimension, and is tuned for speed, a property that is strongly influenced by the temporal delay (Zanker et al., 1999). If one assumes a half-correlator that is sampling across a particular spatial dimension (its PD-ND axis) in a two dimensional space, changing the angle of the moving stimulus relative to the fixed orientation of the input channels will shift the temporal offset between when an edge reaches the two inputs. Consider the example of an edge moving orthogonal to its long axis (Figure 7G). When the direction of motion at constant velocity is aligned with the axis defined by the two inputs to the motion detector, the temporal delay between the arrival of the edge at each input channel is maximal. If the direction of motion of the edge is rotated relative to this axis, different points along the edge will make contact with the input channels and, as a

result, the time difference between when the edge arrives at the first input channel relative to the second channel will be shorter than the maximal value for the same speed of motion. In this manner, edges moving at acute angles to the axis of motion detection will appear to the correlator as if they are moving faster than their true speed (Figure 7G). In an extreme example, when the direction of motion is nearly orthogonal to the axis of the motion detector, the edge arrives nearly simultaneously at the two inputs and thus appears to be moving very quickly. This obligate relationship between speed and direction of motion makes the prediction that if only the motion axis and not other features of the spatial receptive field are engaged to determine directional tuning, then speed tuning in the PD should completely determine directional tuning. Conversely, if a motion detector were to utilize 2-dimensional spatial information, such as that provided by an OS spatial receptive field, the directional tuning curve would be different than that predicted by the speed tuning.

To test whether the two-dimensional components of T4 and T5 spatial receptive fields alter directional tuning, we first measured speed tuning responses to a square wave grating with a 20° spatial period at speeds ranging from 5°/s to 150°/s (Figure S7A). We found that speed tuning peaks around 20°/s, consistent with previous reports (Figure S7B, Maisak et al. 2013). We then used these speed tuning measurements to calculate the predicted directional tuning width for a grating moving at 20°/s (Figure 7G, Figure S7A). For example, an edge moving at 50 °/s along the PD of the detector would produce the same temporal offset between the arrival times at the two input channels as an edge that is moving at 20°/s that is tilted by an angle of 66° away from the preferred axis (Figure 7G). Thus, responses evoked by a grating moving 50 °/s in the PD were used to predict the magnitude of response to a motion stimulus tilted 66° away from the PD (Figure 7G, Figure S7A). Similarly, a moving edge tilted by 90° relative to the detector axis would hit both inputs simultaneously and elicit no motion response. Strikingly, for Layers A-C, the directional tuning curves predicted by the speed sensitivity of the detectors were significantly broader than our direct measurements of the true directional tuning curves (Figure 7H, Figure S7). This difference was not significant for Layer D, which notably also had the widest predicted tuning curve. This analysis demonstrates that information about speed tuning alone poorly predicts tuning width for T4 and T5, suggesting that receptive field features independent of the motion axis affect direction selectivity. We propose that the circuitry that produces orientation selectivity sharpens the directional tuning curve by suppressing motion responses to stimuli that are tilted away from the preferred axis, thereby stimulating a larger portion of the antagonistic surround (Figure 8).

DISCUSSION

Previous studies demonstrated that T4 and T5 are DS, with a specific subtype of each cell responding preferentially to motion in one of the four cardinal directions (Maisak et al., 2013). This finding suggested that T4 and T5 and their inputs represent elementary motion detecting circuits, but left open the algorithmic mechanism by which these local motion detectors become DS. Our data demonstrate that supra-linear summation of inputs that arrive in the PD are critical to the emergence of elementary motion signals in T4 and T5 dendrites, as predicted by HRC and motion energy models. We also discover an unexpected property of these motion detectors. In particular, T4 and T5 neurons display prominent responses to

static visual stimuli that are OS and display an antagonistic spatial surround. Asymmetric inhibitory sub-regions within the T4 and T5 spatial receptive field could explain both orientation selectivity and surround antagonism. Consistent with this idea, inhibitory signaling is required for both response properties. Notably, both orientation selectivity and direction selectivity manifest themselves in individual T4 and T5 cells and are specifically correlated such that orientation tuning is orthogonal to the axis of direction preference. Thus, the motion detector becomes selective for a particular oriented edge and the direction for which that edge will produce the greatest motion energy. As a result, directional tuning is narrower than the measured speed tuning profile of T4 and T5 would predict. We therefore propose that the same antagonistic receptive field properties that produce orientation selectivity sharpen the selectivity of each T4 and T5 subclass for motion in a particular direction.

Direction selective signals arise within T4 and T5 dendrites

Previous studies suggested that T4 and T5 are the most peripheral neurons in the visual system to display direction selectivity (Maisak et al., 2013). In contrast, significant feed-forward inputs onto T4 and T5 do not display direction selectivity (Behnia et al., 2014; Shinomiya et al., 2014; Strother et al., 2014; Takemura et al., 2013). These retinotopic columnar inputs display spatially asymmetric wiring onto individual T4 and T5 dendrites that correlates with the axis of directional preference (Shinomiya et al., 2014; Takemura et al., 2013). In addition, these cells also have different temporal response profiles that depend on cell type (Behnia et al., 2014; Meier et al., 2014; Strother et al., 2014). Thus, these presynaptic inputs could generate both the spatial offset and temporal delays necessary for the motion computation as they converge onto T4 and T5 dendrites. Consistent with this notion, select fibers of passage within the inner chiasm display DS responses to moving gratings, suggesting that dendrites might also be directionally tuned (Maisak et al., 2013). Our data demonstrate that calcium signals within both T4 and T5 dendrites are, in fact, DS, thereby identifying the neuronal compartment that implements the core motion computation (Figure 1). Establishing the extent to which these dendritic calcium signals are generated by voltage-gated channels, ligand gated receptors or intracellular stores would strongly constrain the molecular and biophysical mechanisms that underlie this paradigmatic neural computation.

Selective amplification enhances preferred direction signals

What algorithms compute motion direction within T4 and T5 dendrites? All motion detecting circuits must compare signals across space and time. This computation can be implemented either by amplifying motion signals that arrive in the PD, as described by the HRC, or by suppressing signals that arrive in the ND, as in the B-L model. Here we show that PD amplification occurs within T4 and T5 dendrites. Local apparent motion stimuli that simulate the motion of an edge in the PD evoked larger responses than either ND motion or sequential flashes (Figures 2, 3). These PD responses were larger than the linear sum of responses evoked by the individual static components of the stimulus, suggesting that the appropriate coincidence of visual inputs leads to selective amplification of a motion signal. Both T4 and T5 utilize such nonlinear amplification, arguing that both ON and OFF motion detectors use broadly similar algorithms to achieve direction selectivity (Figures 2, 3).

However, T5 but not T4 showed ND responses that were smaller than the linear prediction, which could be the result of contrast adaptation. Taken together with previous studies of the presynaptic inputs to T4 and T5, our data are consistent with a model where spatially offset and temporally delayed excitatory synaptic inputs converge onto T4 and T5 dendrites such that PD signals interact and become amplified. A wealth of data measuring behavioral and neural outputs of motion detecting circuitry has argued strongly that motion detecting circuits in flies implement a HRC (reviewed in Borst, 2014). Here we measured the direct output of the elementary motion detector itself and demonstrate for the first time that T4 and T5 perform non-linear amplification.

The mechanistic underpinnings of direction selectivity have been studied extensively in the vertebrate retina. Early characterization of DS ganglion cells provided support for a B-L model, as ON-OFF DS ganglion cells receive strong GABAergic inhibition during ND motion (Barlow and Levick, 1965; Fried et al., 2002, 2005). More recent studies argue that direction selectivity emerges within the dendrites of starburst amacrine cells (Euler et al., 2002). One hypothesis for how these signals arise draws direct parallels with the circuit motif seen in the fly elementary motion detector. In this model, the temporal delays required for the motion computation arise presynaptic to the DS neuron, through a difference in temporal filtering of different bipolar cell subtypes (Baden et al., 2013; Borghuis et al., 2013; Kim et al., 2014). In turn, differential asymmetric wiring of these bipolar cell subtypes onto distinct locations along the starburst amacrine cell dendrite creates a spatial offset that is consistent with the observed direction selectivity (Kim et al., 2014). Alternate models have proposed that passive signal conduction along the dendrite could also provide the necessary temporal delay (Tukker et al., 2004). The much shorter dendrites of T4 and T5 make it unlikely that conduction delays have a dramatic impact on signal timing (Shinomiya et al., 2014; Takemura et al., 2013), but postsynaptic receptors with different signaling kinetics could contribute to the relative timing of the synaptic inputs (Shinomiya et al., 2014).

Orientation selectivity arises early within visual processing

In addition to direction selectivity, T4 and T5 display orientation selectivity for static stimuli. This OS is not a trivial product of the spatially offset presynaptic inputs that have been suggested by anatomical reconstruction to support motion detection, as the pattern of these inputs would predict a spatial orientation that is aligned with the axis of directional preference, contrary to our observations (Takemura et al., 2013). This OS is also consistent with previously reported responses of T4 and T5 to a stimulus with opposing motion signals (Maisak et al., 2013). Orientation tuning has previously been described in the central complex of the fruit fly brain (Seelig and Jayaraman, 2013). This work posited that orientation tuning might emerge in this deep, sensorimotor brain region to facilitate visually guided behavior. We show that orientation tuning emerges early in visual processing, in T4 and T5 (Figure 4). It is an open question whether the orientation tuning observed in the central complex is inherited from these cells, or if these features are extracted *de novo* at a later processing stage. Nonetheless, the emergence of these V1-like response properties so early in visual processing streams dramatically revises the accepted view of visual circuit organization in *Drosophila*.

Inhibitory signaling produces orientation selectivity and surround antagonism

In primary visual cortex orientation selectivity emerges from a combination of elongated excitatory and inhibitory sub-regions within the spatial receptive field (Hubel and Wiesel, 1962). Similarly, T4 and T5 receptive fields also harbor a surround region that suppresses visual responses. Notably, this antagonism was strong enough to completely abolish responses to full field illumination (Figure 4 and Maisak et al., 2013). Intriguingly, when we systematically rotated gratings from the preferred angle to the orthogonal, non-preferred angle, we observed a reduction in response of approximately the same magnitude as this surround antagonism (Figure 4). This argues that the same inhibitory mechanism produces both orientation selectivity and surround antagonism. Consistent with this idea, GABA-A receptor signaling is required for both of these receptive field properties (Figure 5). A number of the neurons upstream of T5 have antagonistic center surround organizations (Freifeld et al., 2013; Meier et al., 2014; Strother et al., 2014). Thus it seems likely that the construction of inhibitory sub-regions in the receptive fields of T4 and T5 is distributed across the circuit, perhaps in a manner similar to how center surround inputs from the Lateral Geniculate Nucleus create the excitatory and inhibitory sub-regions of V1 simple cells (Hubel and Wiesel, 1962). We note that inhibitory signaling has many effects on the response properties of T4 and T5, including disrupting direction selectivity through effects on both spatial and temporal filtering, results that are consistent with earlier observations of downstream motion-sensitive neurons (Figure 6, Figure S6; Schmid and Bülthoff 1988). Thus, inhibitory signaling plays a vital role in supporting both orientation tuning and motion processing.

Orientation selectivity sharpens directional tuning

Remarkably, T4 and T5 not only display direction tuning and orientation selectivity, but the axes of these features are orthogonal (Figure 7). Edges create the strongest motion signal when moving in the direction orthogonal to their long axes. As a result, the combination of OS and DS tuning properties observed in T4 and T5 means that these neurons are most selective for an object or edge that is likely to move in that neuron’s PD. To investigate if the circuits that produce orientation selectivity in T4 and T5 might also impact directional responses, we compared our measured directional tuning with the predictions made by models of motion detection that only detect motion along a single linear axis. We used this interaction to predict directional tuning based solely on experimental measurements of speed tuning in T4 and T5. Strikingly, the true directional tuning curves of T4 and T5 were narrower than this prediction.

How does the spatiotemporal receptive field of T4 and T5 shape the motion computation? Interesting insight regarding the interaction between an oriented receptive field and direction selectivity comes from comparing the directional tuning of DS retinal ganglion cells, which do not display a systematic orientation preference, to simple cells in visual cortex that have strong orthogonal orientation tuning (DeAngelis et al., 1995; He et al., 1998). These two circuits display dramatic differences in the width of their directional tuning, with V1 simple cells being much more tightly tuned than retinal ganglion cells (Elstrott et al., 2008; Henry et al., 1974; Hubel and Wiesel, 1959). Thus OS and DS interactions can, at least partially, account for this difference in tuning across these different motion-detecting circuits. One

consequence of an orthogonal relationship between OS and DS response properties is that the inhibitory circuitry that produces orientation selectivity could sharpen directional tuning by reducing responses to edges moving at angles slightly different from the PD. In this view, the center-surround mechanism that generates orientation selectivity within T4 and T5 suppresses responses to non-optimally oriented bars or edges, because they activate a larger portion of the antagonistic surround. This makes the circuit more selective to moving stimuli that are optimally oriented and narrows directional tuning (Figure 8). Thus, much like V1 simple cells, the asymmetric receptive field structure of T4 and T5 is poised to provide this additional layer of selectivity for motion direction.

We propose that T4 and T5 perform selective amplification of PD signals at the receptive field center and utilize spatially asymmetric surround inhibition to sharpen directional tuning. Thus, the simultaneous encoding of these two higher order visual features, namely motion direction and orientation, shapes motion processing in T4 and T5. The analogy between elementary motion detectors in the fly and cells in the vertebrate visual cortex is striking: such a similar neural representation must reflect a fundamental and advantageous circuit architecture for motion processing.

EXPERIMENTAL PROCEDURES

In vivo calcium imaging experiments were performed on a Leica SP5 two photon microscope, using 920nm light from a Chameleon Vision II laser. GCaMP6f was expressed in T4 and T5 using the $T4/T5^{GMR42F06}Gal4$ driver, in the T4 subtype that innervates lobula plate layer C using $T4^{GMR54A03}Gal4$, and stochastically in T5 and T4 in a clonal approach using hsFlp to excise Gal80 from a tub FRT Gal80 FRT construct, combined with *UAS-GCaMP6f* and $T4/T5^{GMR42F06}Gal4$. GABAergic signaling was inhibited by pharmacological application of 5 μM picrotoxin. Experiments were either performed in wild type or in the PTX insensitive Rdl background Rdl^{1}/Rdl^{MDRR}. See Supplemental Experimental Procedures for detailed methods.

Supplementary Material

Refer to Web version on PubMed Central for supplementary material.

ACKNOWLEDGEMENTS

We would like to thank Nirao Shah, Lisa Giocomo, Anthony Movshon, Eric Trautmann and all of the members of the Clandinin Laboratory for valuable comments on the manuscript and Jesse Lipp for assistance with statistical analysis. Y.E.F. was supported by a National Science Foundation Fellowship, M.S. was supported by a postdoctoral fellowship from the Jane Coffin Childs Memorial Fund for Medical Research. This work was funded by a National Institutes of Health R01 EY 022638 (T.R.C).

REFERENCES

Adelson EH, Bergen JR. Spatiotemporal energy models for the perception of motion. J. Opt. Soc. Am. 1985; 2:284–299.

Ammer G, Leonhardt A, Bahl A, Dickson BJ, Borst A. Functional Specialization of Neural Input Elements to the Drosophila ON Motion Detector. Curr. Biol. 2015:1–7. [PubMed: 25532895]

Baden T, Berens P, Bethge M, Euler T. Spikes in mammalian bipolar cells support temporal layering of the inner retina. Curr. Biol. 2013; 23:48–52. [PubMed: 23246403]

Barlow HB, Levick WR. The Mechanism of Directionally Selective Units in the Rabbit Retina. J. Physiol. 1965; 178:477–504. [PubMed: 5827909]

Behnia R, Clark DA, Carter AG, Clandinin TR, Desplan C. Processing properties of ON and OFF pathways for Drosophila motion detection. Nature. 2014; 512:427–430. [PubMed: 25043016]

Borghuis BG, Marvin JS, Looger LL, Demb JB. Two-Photon Imaging of Nonlinear Glutamate Release Dynamics at Bipolar Cell Synapses in the Mouse Retina. J. Neurosci. 2013; 33:10972–10985. [PubMed: 23825403]

Borst A. In search of the holy grail of fly motion vision. Eur. J. Neurosci. 2014; 40:3285–3293. [PubMed: 25251169]

Buchner E, Buchner S, Bülthoff I. Deoxyglucose mapping of nervous activity induced in Drosophila brain by visual movement. J Comp Physiol A. 1984; 155:471–483.

Clark DA, Bursztyn L, Horowitz M, Schnitzer MJ, Clandinin TR. Defining the computational structure of the motion detector in Drosophila. Neuron. 2011; 70:1165–1177. [PubMed: 21689602]

DeAngelis GC, Ohzawa I, Freeman RD. Receptive-field dynamics in the central visual pathways. Trends Neurosci. 1995; 18:451–458. [PubMed: 8545912]

Egelhaaf M, Borst A. Are there separate ON and OFF channels in fly motion vision? Vis. Neurosci. 1992; 8:151–164. [PubMed: 1558827]

Elstrott J, Anishchenko A, Greschner M, Sher A, Litke AM, Chichilnisky EJ, Feller MB. Direction Selectivity in the Retina Is Established Independent of Visual Experience and Cholinergic Retinal Waves. Neuron. 2008; 58:499–506. [PubMed: 18498732]

Euler T, Detwiler PB, Denk W. Directionally selective calcium signals in dendrites of starburst amacrine cells. Nature. 2002; 418:845–852. [PubMed: 12192402]

Ffrench-Constant RH, Rocheleau T, Steichen J, Chalmers A. A point mutation in a Drosophila GABA receptor confers insecticide resistance. Nature. 1993; 362:449–451. [PubMed: 8389005]

Fischbach K-F, Dittrich APM. The optic lobe of Drosophila melanogaster . I . A Golgi analysis of wild-type structure. Cell Tissue Res. 1989; 258:411–475.

Freifeld L, Clark DA, Schnitzer MJ, Horowitz MA, Clandinin TR. GABAergic Lateral Interactions Tune the Early Stages of Visual Processing in Drosophila. Neuron. 2013; 78:1075–1089. [PubMed: 23791198]

Fried SI, Münch TA, Werblin FS. Mechanisms and circuitry underlying directional selectivity in the retina. Nature. 2002; 420:411–414. [PubMed: 12459782]

Fried SI, Münch TA, Werblin FS. Directional selectivity is formed at multiple levels by laterally offset inhibition in the rabbit retina. Neuron. 2005; 46:117–127. [PubMed: 15820698]

Gibson, JJ. The perception of the visual world. Boston, MA: 1950.

Gordon MD, Scott K. Motor control in a Drosophila taste circuit. Neuron. 2009; 61:373–384. [PubMed: 19217375]

Gruntman E, Turner GC. Integration of the olfactory code across dendritic claws of single mushroom body neurons. Nat. Neurosci. 2013; 16:1821–1829. [PubMed: 24141312]

Hassenstein V, Reichardt W. [System theoretical analysis of time, sequence and sign analysis of the motion perception of the snout-beetle Chlorophanus]. German. Z. Naturforsch. 1956; 11:513–524.

He S, Levick WR, Vaney DI. Distinguishing direction selectivity from orientation selectivity in the rabbit retina. Vis. Neurosci. 1998; 15:439–447. [PubMed: 9685197]

Henry GH, Bishop PO, Dreher B. Orientation, axis and direction as stimulus parameters for striate cells. Vision Res. 1974; 14:767–777. [PubMed: 4422599]

Hubel DH, Wiesel TN. Receptive Fields of Single Neurones in the Cat's Striate Cortex. J Physiol. 1959; 148:574–591. [PubMed: 14403679]

Hubel DH, Wiesel TN. Receptive Fields, Binocular interaction and Functional Architecture in the Cat's Visual Cortex. J Physiol. 1962; 160:106–154. [PubMed: 14449617]

Joesch M, Schnell B, Raghu SV, Reiff DF, Borst A. ON and OFF pathways in Drosophila motion vision. Nature. 2010; 468:300–304. [PubMed: 21068841]

Kim JS, Greene MJ, Zlateski A, Lee K, Richardson M, Turaga SC, Purcaro M, Balkam M, Robinson A, Behabadi BF, et al. Space - time wiring specificity supports direction selectivity in the retina. Nature. 2014; 509:331–336. [PubMed: 24805243]

Liu WW, Wilson RI. Glutamate is an inhibitory neurotransmitter in the Drosophila olfactory system. Proc. Natl. Acad. Sci. U. S. A. 2013; 110:10294–10299. [PubMed: 23729809]

Maisak MS, Haag J, Ammer G, Serbe E, Meier M, Leonhardt A, Schilling T, Bahl A, Rubin GM, Nern A, et al. A directional tuning map of Drosophila elementary motion detectors. Nature. 2013; 500:212–216. [PubMed: 23925246]

Mauss AS, Meier M, Serbe E, Borst A. Optogenetic and Pharmacologic Dissection of Feedforward Inhibition in Drosophila Motion Vision. J. Neurosci. 2014; 34:2254–2263. [PubMed: 24501364]

Meier M, Serbe E, Maisak MS, Haag J, Dickson BJ, Borst A. Neural Circuit Components of the Drosophila OFF Motion Vision Pathway. Curr. Biol. 2014; 24:385–392. [PubMed: 24508173]

Niell CM, Smith SJ. Functional imaging reveals rapid development of visual response properties in the zebrafish tectum. Neuron. 2005; 45:941–951. [PubMed: 15797554]

Niell CM, Stryker MP. Highly selective receptive fields in mouse visual cortex. J. Neurosci. 2008; 28:7520–7536. [PubMed: 18650330]

Schmid A, Bülthoff H. Using Neuropharmacology to Distinguish between Excitatory and Inhibitory Movement Detection Mechanisms in the Fly Calliphoa erythrocephala. Biol. Cybern. 1988; 80:71–80.

Seelig JD, Jayaraman V. Feature detection and orientation tuning in the Drosophila central complex. Nature. 2013; 503:262–266. [PubMed: 24107996]

Shinomiya K, Karuppudurai T, Lin T-Y, Lu Z, Lee C-H, Meinertzhagen IA. Candidate Neural Substrates for Off-Edge Motion Detection in Drosophila. Curr. Biol. 2014; 24:1062–1070. [PubMed: 24768048]

Silies M, Gohl DM, Fisher YE, Freifeld L, Clark DA, Clandinin TR. Modular Use of Peripheral Input Channels Tunes Motion-Detecting Circuitry. Neuron. 2013; 79:111–127. [PubMed: 23849199]

Strother JA, Nern A, Reiser MB. Direct observation of ON and OFF pathways in the Drosophila visual system. Curr. Biol. 2014; 24:976–983. [PubMed: 24704075]

Takemura S, Bharioke A, Lu Z, Nern A, Vitaladevuni S, Rivlin PK, Katz WT, Olbris DJ, Plaza SM, Winston P, et al. A visual motion detection circuit suggested by Drosophila connectomics. Nature. 2013; 500:175–181. [PubMed: 23925240]

Tukker JJ, Taylor WR, Smith RG. Direction selectivity in a model of the starburst amacrine cell. Vis. Neurosci. 2004; 21:611–625. [PubMed: 15579224]

Zanker JM, Srinivasan MV, Egelhaaf M. Speed tuning in elementary motion detectors of the correlation type. Biol. Cybern. 1999; 80:109–116. [PubMed: 12440388]

HIGHLIGHTS

- Direction selectivity arises in T4 and T5 dendrites
- T4 and T5 amplify preferred direction signals
- Orientation selectivity in T4/T5 is orthogonal to the axis of motion detection
- Inhibition is required for orientation selectivity and directional tuning

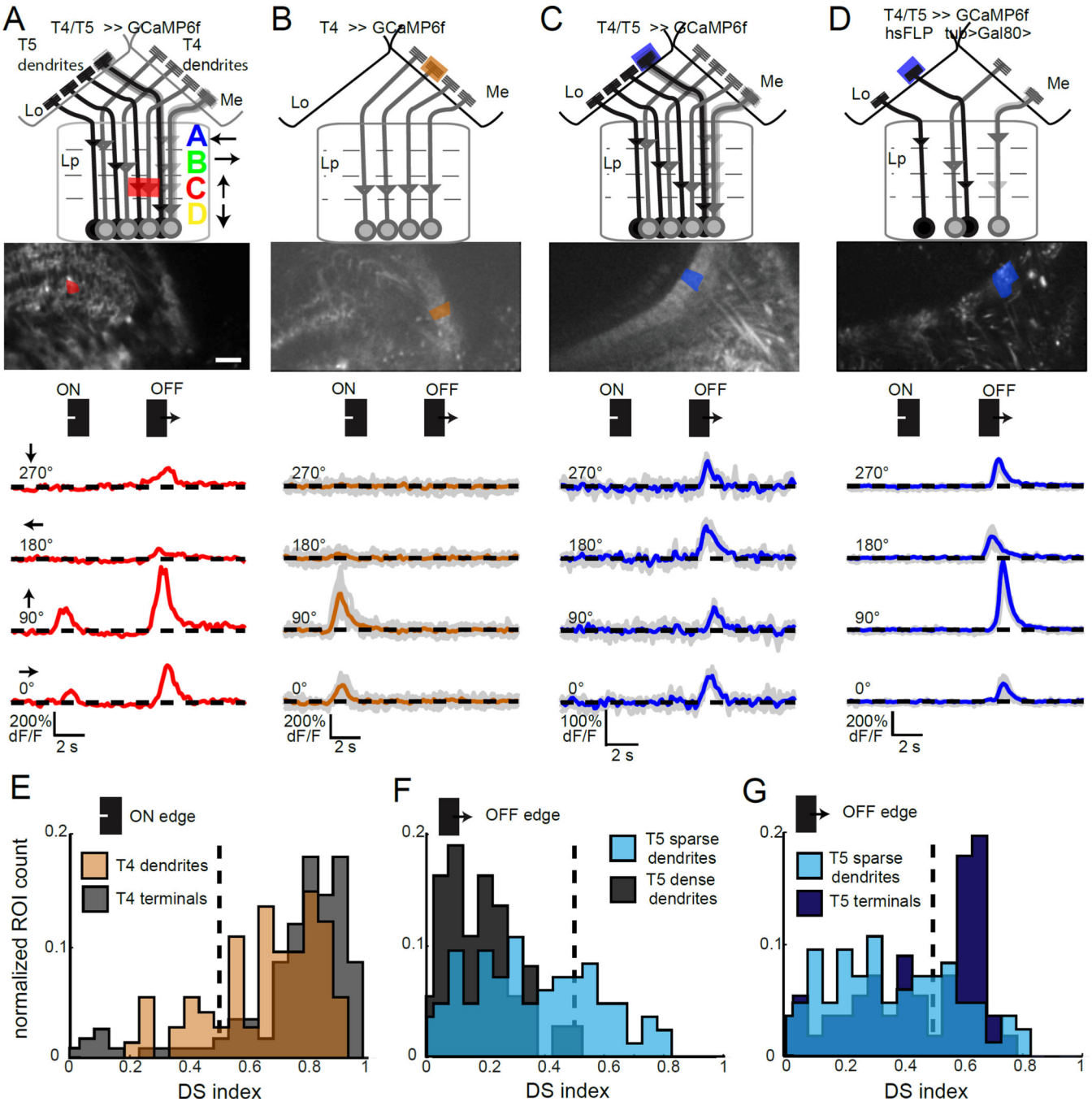

Figure 1. The dendrites of T4 and T5 are directionally tuned

(A–D) Schematic of the T4 and T5 projection area, corresponding to the maximum intensity projection shown below, including the proximal medulla (Me), the lobula (Lo) and the lobula plate (Lp) with its four layers A–D (Maisak et al., 2013). Scale bar is 15 μm. A single region of interest (ROI) analyzed to extract the trace below is shaded. Traces display *in vivo* calcium responses to moving ON and OFF edges to one presentation of the stimulus **(A)** or the mean trace to repeated stimulus presentations, with individual response traces in grey **(B–D)**. **(E–G)** Histograms plotting the normalized ROI count observed at each DS index

value. Sample size (N = number of flies (ROIs)) was N = 12 (117) for T4 terminals in lobula plate layer C and N = 13 (74) for T4 dendrites in the proximal medulla **(E)**, N = 13 (84) sparse T5 dendrites and N = 6 (37) dense T5 dendrites in **(F)** and N = 13 (84) sparse T5 dendrites and N = 10 (56) T5 axon terminals in layer C of the lobula plate **(G)**. See also Figure S1.

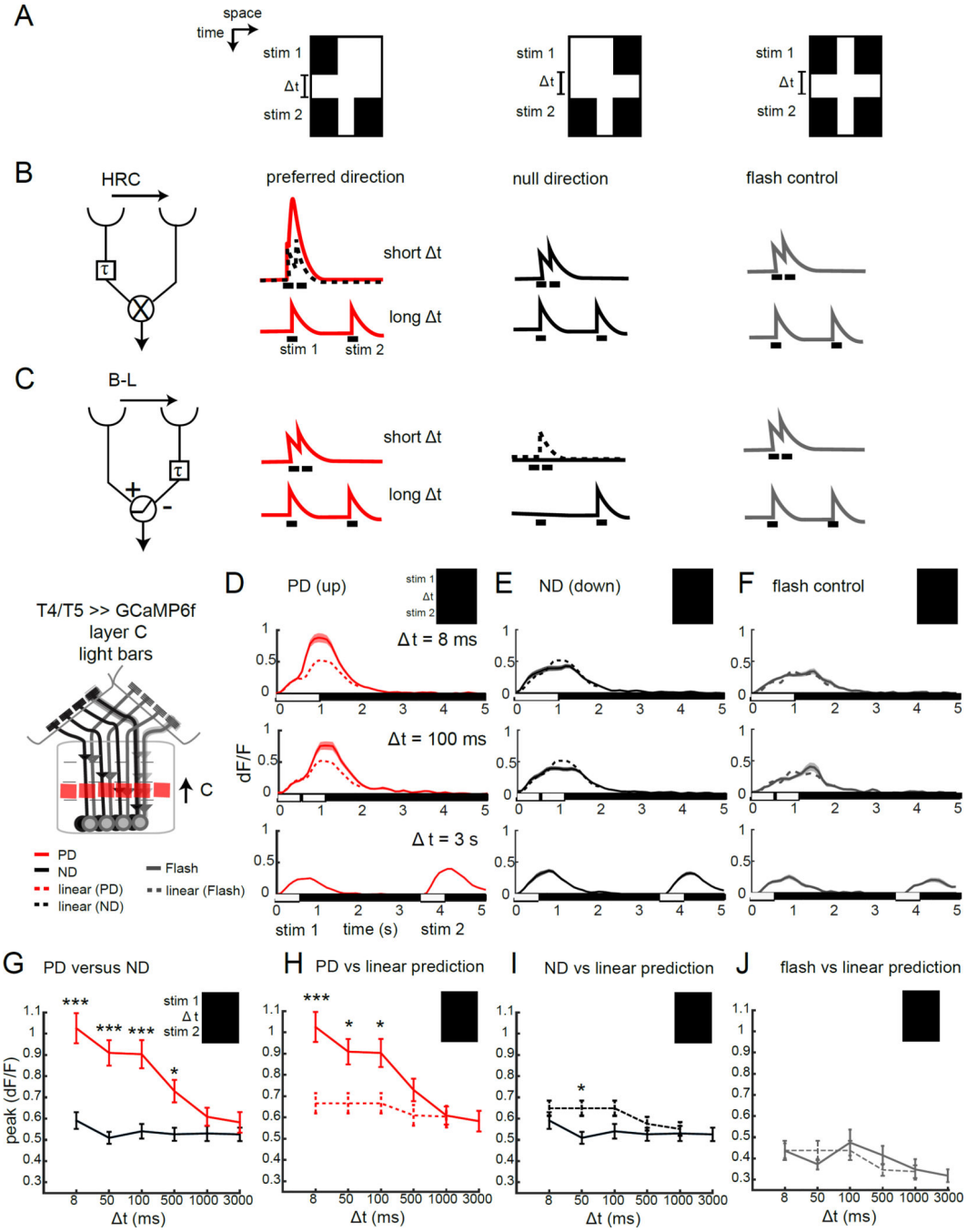

Figure 2. T4 responses selectively enhance preferred direction signals

(A) X-T plots of apparent motion stimuli. A single bar appears for 0.5 s (stim 1); followed by a temporal delay of variable length (Δt), then a pair of bars appears for 0.5 s (stim 2). Shown are bar pair stimuli that create apparent motion to the right (PD), apparent motion to the left (middle panel, ND) and a control in which two pairs of bars are separated by Δt (flash control). **(B,C)** HRC and B-L models that are tuned to rightward motion, and their predicted responses to the stimuli shown in **(A)**. The dotted lines display the linear prediction based on the sum of individual stim 1 and stim 2 responses. **(D–F)** Calcium

signals imaged in the axon terminals of T4 and T5 in lobula plate layer C in response to a light bar version of the stimuli described above, at three different temporal delays. The dotted line represents the linear prediction based on the separate responses (recorded at Δt = 3 s). N = 14 (67) for axon terminals in **(D, E)** and N = 4(16) in **(F). (G–J)** Quantification of the peak calcium response at various time delays, comparing PD and ND responses **(G)**, PD responses and the linear prediction **(H)**, ND responses and the linear prediction **(I)** and double flash control responses with the linear prediction **(J)**, for axon terminals of T4 and T5 in layer C of the lobula plate. * $p < 0.05$, *** $p < 0.001$, unpaired two tailed Student's t-test with Bonferroni correction for multiple comparisons. See also Figure S2.

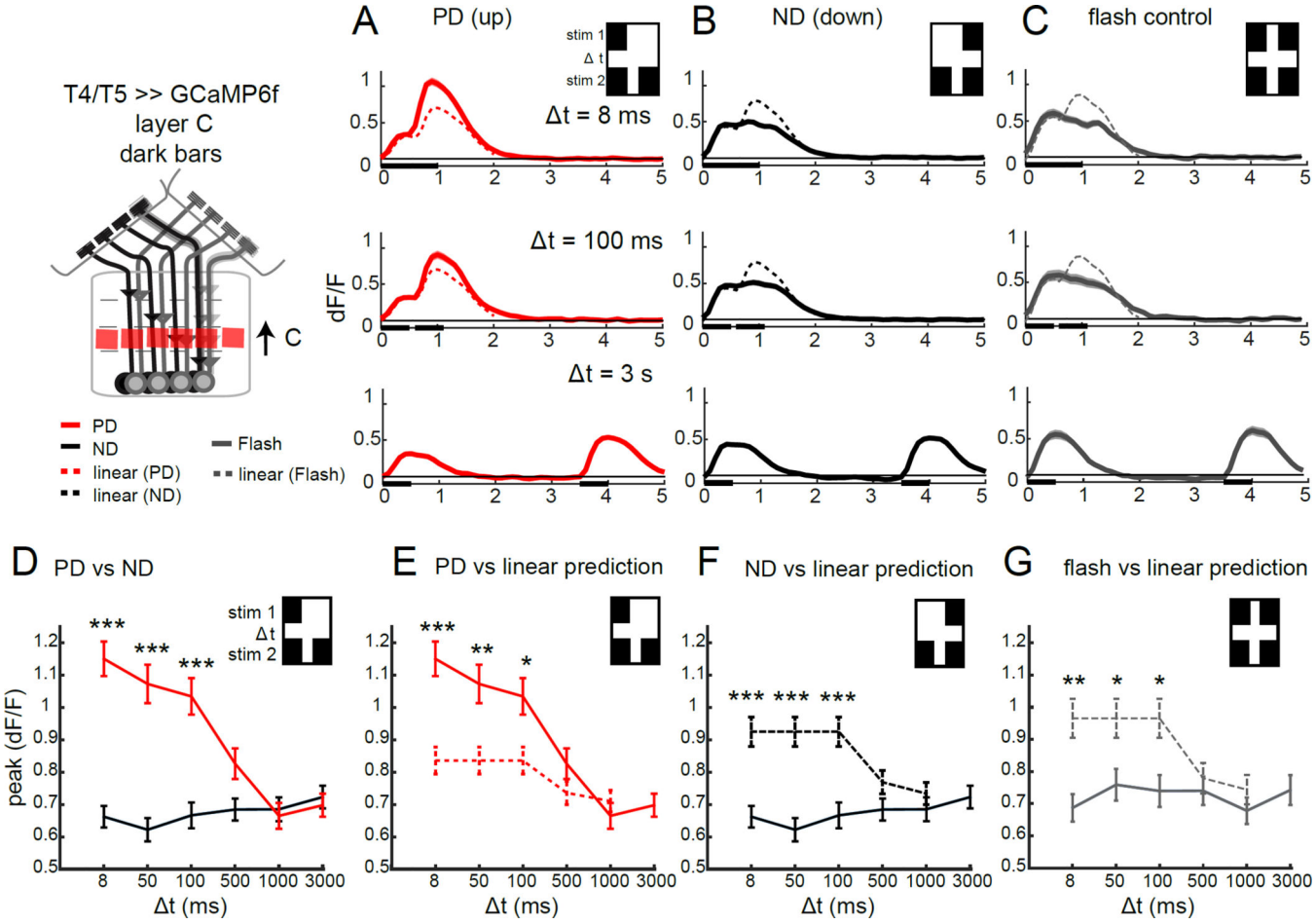

Figure 3. T5 responses selectively enhance preferred direction signals

(A–C) Calcium signals imaged in the axon terminals of T4 and T5 in lobula plate layer C in response to a dark bar version of the stimuli described in Figure 2, at three different temporal delays. The dotted line represents the linear prediction based on the separate responses (recorded at Δt = 3 s). N = 21 (114) for axon terminals in **(A,B)** and N = 6 (35) in **(C). (D–G)** Quantification of the peak calcium response at various time delays, comparing PD and ND responses **(D)**, PD responses and the linear prediction **(E)**, ND responses and the linear prediction **(F)** and double flash control responses with the linear prediction **(G)**, for axon terminals of T4 and T5 in layer C of the lobula plate. * p <0.05, **p<0.01, *** p<0.001, unpaired two tailed Student's t-test with Bonferroni correction for multiple comparisons. See also Figure S3.

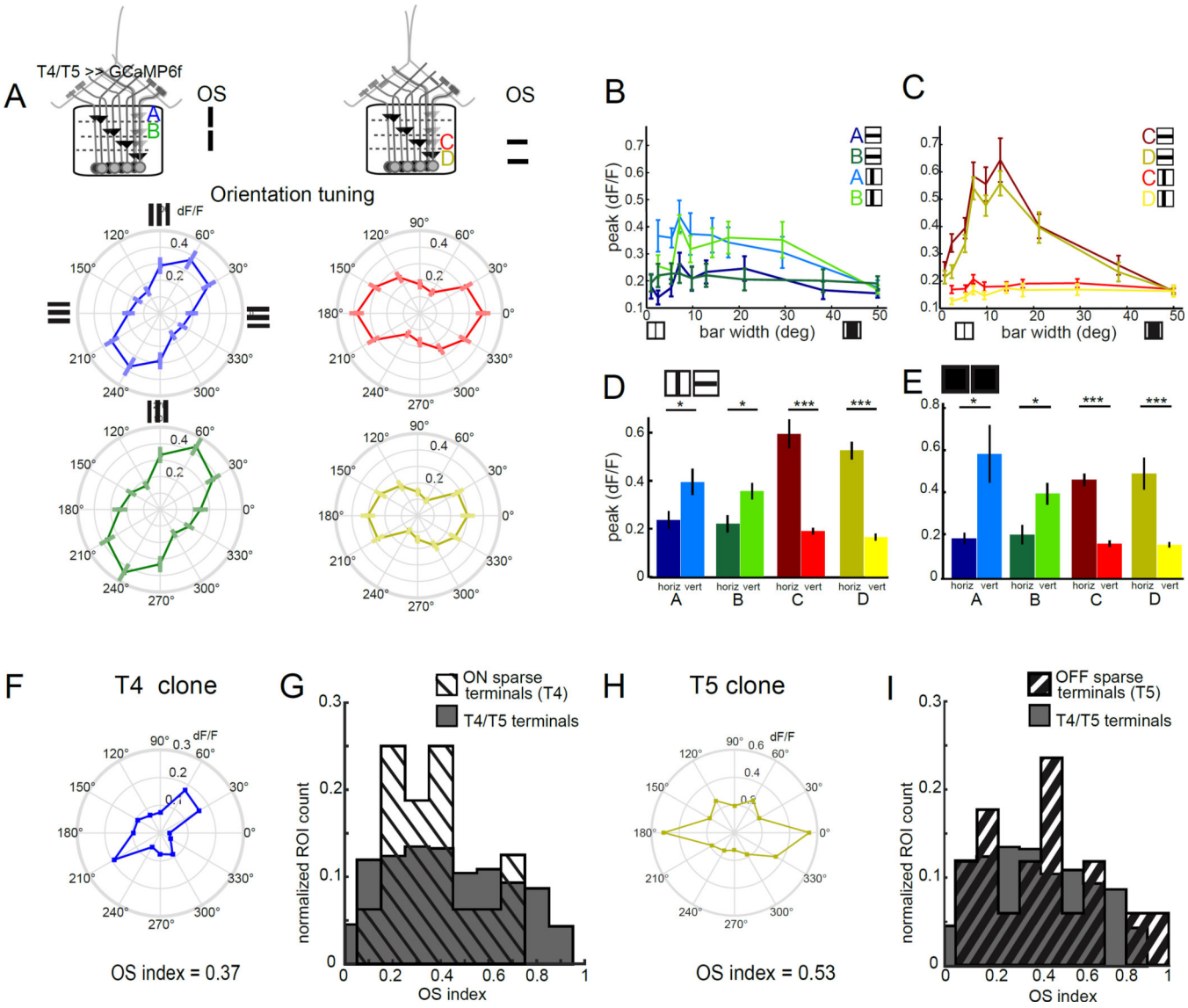

Figure 4. Individual T4 and T5 neurons are orientation tuned and exhibit surround antagonism

(A) Polar plots displaying mean calcium responses in T4 and T5 axon terminals to static gratings of different orientations. Error bars are ±SEM. Layer A: N = 9(75), layer B: N = 9 (69), layer C: N = 9 (96), layer D: N = 9(78). **(B,C)** Peak calcium responses to horizontally or vertically oriented dark bars of variable width, imaged in T4 and T5 axon terminals in lobula plate layer A (N = 5 (9)) and layer B (N = 4 (10)) or layer C (N = 7 (38)) and layer D (N = 7 (25)). **(D,E)** Quantification of the difference in peak responses to horizontally and vertically oriented dark bars that were 7 to 15° wide **(D)** or light bars that were 5 to 10° wide **(E)**, using averaged peak responses of the same ROIs as in panels **(B,C)** and Figure S4 B,C. * $p<0.05$, *** $p<0.001$, two tailed Student's t-test. **(F,H)** Polar plots showing the mean calcium responses of a single T4 **(F)** or single T5 **(H)** cell. These same ROIs displayed direction tuning to 180° (T4) and 270° (T5) and thus represent putative layer A and D terminals, respectively (see Figure S4). **(G,I)** Normalized histogram comparing orientation selectivity index by ROI for clones with strong DS tuning for ON edges **(G)** or OFF edges

(I) with ROIs obtained using the full T4/T5 GAL4 driver line. Individual clones were selected based on having a DS index > 0.5 for either moving ON or OFF edges respectively. Sample sizes were N = 4(16) flies (ROIs) for ON clones, N = 4 (17) for OFF clones and N = 9 (458) for the full T4/T5 pattern. See also Figure S4.

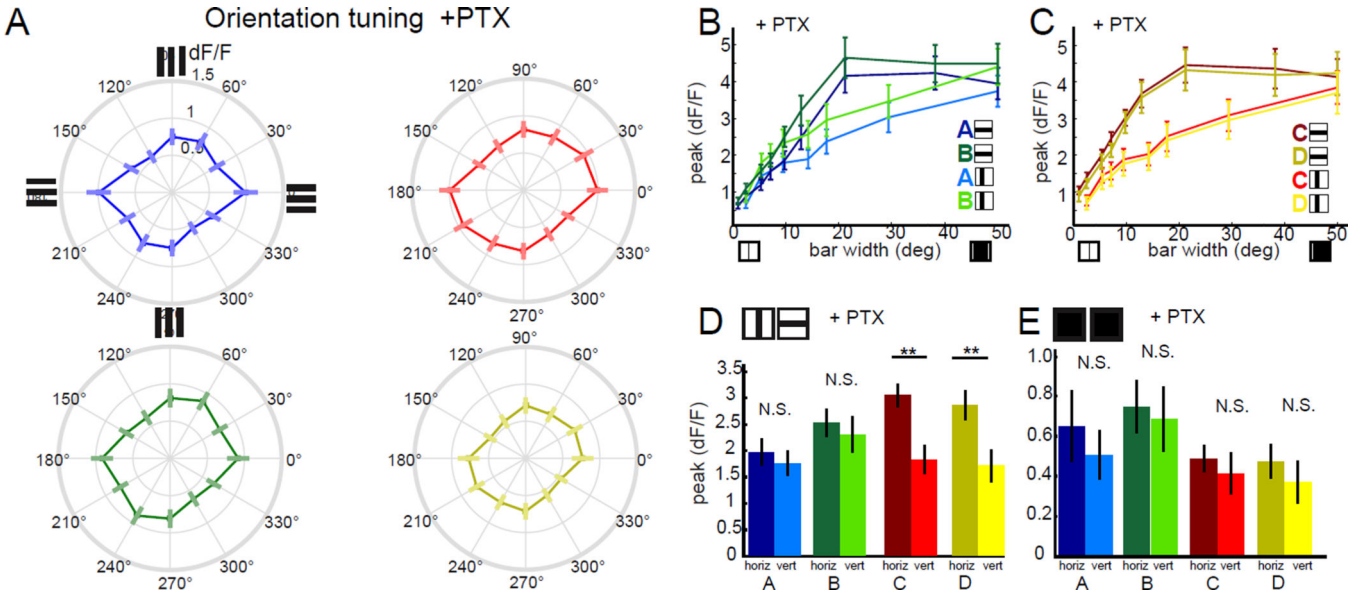

Figure 5. Orientation selectivity and antagonist surround require GABAergic signaling

(A) Polar plots displaying peak calcium responses in T4 and T5 axon terminals to static gratings of different orientations after application of the $GABA_AR$ antagonist picrotoxin (PTX). Error bars are ±SEM. Layer A: N= 4(33). Layer B: N = 4(35). Layer C: N = 4(39). Layer D: N = 4(34). **(B,C)** Peak calcium responses in T4 and T5 axon terminals to static dark bars of various widths, after application of PTX, comparing horizontally and vertically oriented bars. N = 4 (20) for lobula plate layer A. N = 4 (24) for layer B. N = 4 (24) for layer C. N = 4 (22) for layer D. **(D,E)** Quantification of the difference in response to horizontally and vertically oriented dark bars that were 7 to 15° wide **(D)** or light bars that were 5 to 10° wide **(E)** after application of PTX, using averaged peak responses of the same ROIs used in panels **(B,C)** or in Figure S5 B,C. ** $p<0.01$, N.S. = not significant $p>0.05$, two tailed Student's t-test. See also Figure S5.

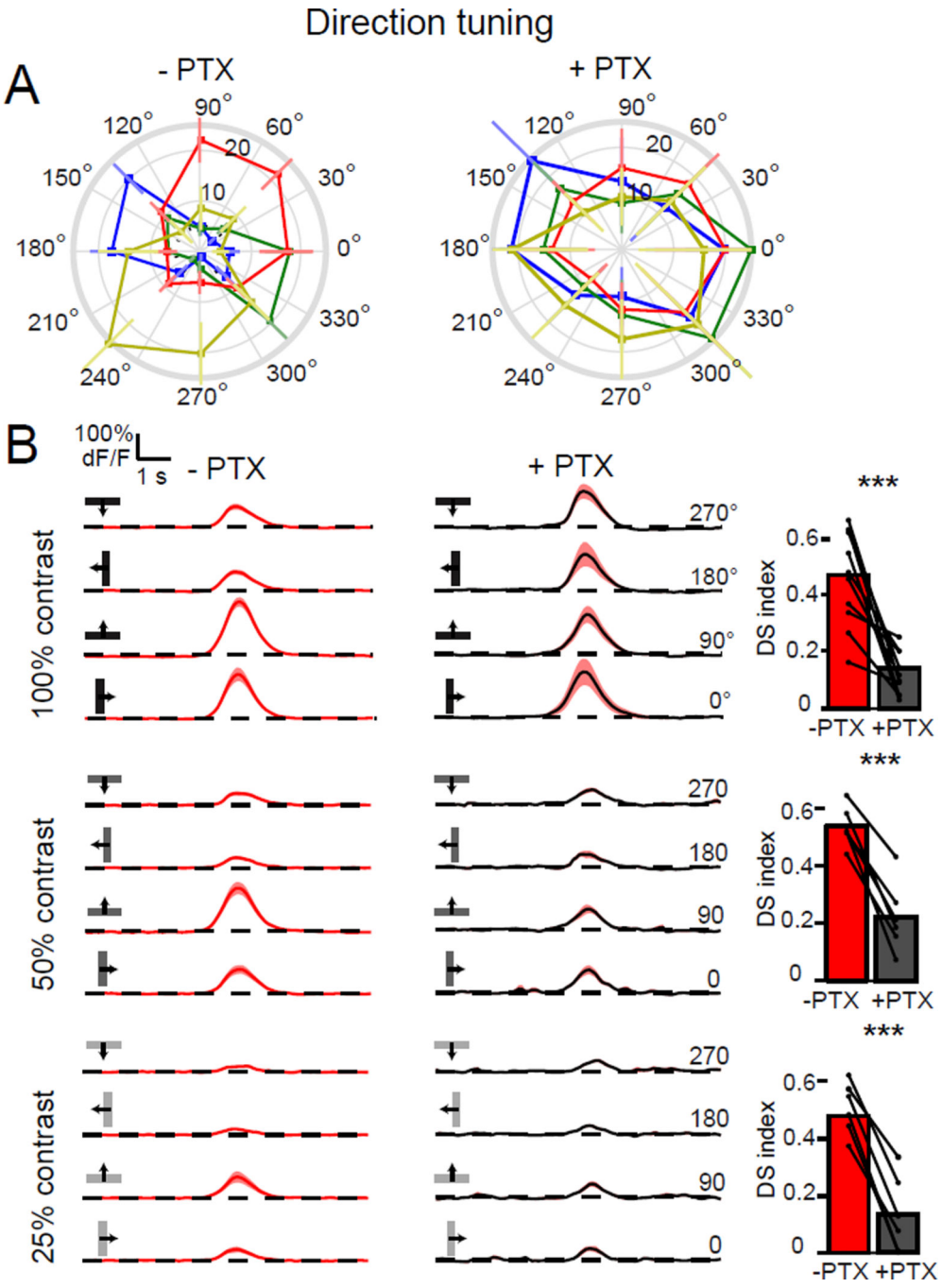

Figure 6. Directionally tuned responses require GABAergic signaling

(A) Polar plots of calcium responses in T4 and T5 axon terminals to a moving dark bar, before and after application of PTX. Plots display the mean integrated responses to the bar moving in one of eight directions. Layers are color-coded: A = blue, B = green, C =red and D = yellow. Error bars are ±SEM. **(B)** Traces display mean responses. Shaded areas are ±SEM. The bar plots quantify the DS indices of these responses before and after PTX application to a moving dark bar at 100% contrast (upper plots). N = 10 flies; 50% contrast

(middle plots), N = 6 flies; 25% contrast (lower plots), N = 6 flies. *** $p<0.001$, two tailed paired Student's t-test. See also Figure S6.

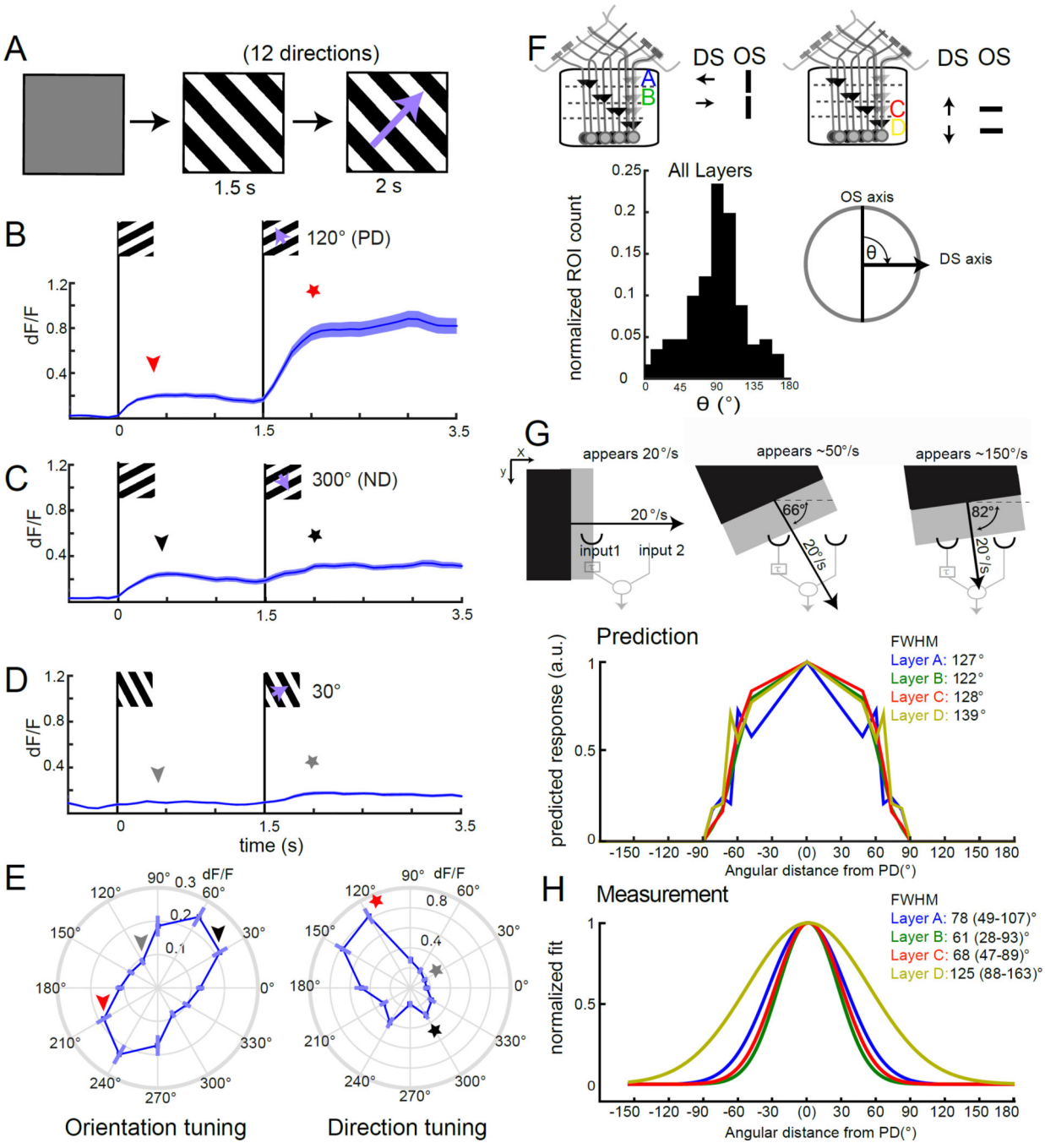

Figure 7. OS and DS tuning properties are orthogonal

(A) Schematic of the stimulus design. Following an initial gray period, a static grating with a 20° spatial period appears at a particular orientation for 1.5 s. Then the grating moves orthogonal to the static pattern at 20°/s in one of 12 directions for 2 s. **(B–D)** Traces of mean calcium responses of T4 and T5 axon terminals of layer A in response to PD (120°) in **(B)**, ND (300°) in **(C)** and an intermediate direction (30°) in **(D)**. Shaded area is ±SEM. **E**, Polar plots displaying peak calcium responses of axon terminals in layer A to static gratings (reflecting orientation tuning) and to moving gratings (reflecting direction tuning). N =

14(108). The stars and arrowheads illustrate which epochs in **(B–D)** correspond to the values in **(E). (F)** Schematic illustration of the relationship between direction selectivity and orientation tuning in each of the four layers of the lobula plate. Histogram plotting the normalized ROI count for the angle θ between the OS and DS vector, ROIs were included in the analysis if they had sufficiently strong and DS responses to the moving grating (see Supplemental Experimental Procedures for details) (N ROIs = 171). **(G)** Schematic illustrating that the speed of a moving edge that is detected by a correlator will vary with motion direction. Predicted tuning width for T4 and T5 axon terminals calculated using measurements of PD responses to a grating moving at speeds ranging from 20°/s to 150°/s. **(H)** Gaussian fits to the measured tuning width of T4 and T5 axon terminals, normalized to the maximum response direction. Layer A: N = 14(108). Layer B: N = 15(106). Layer C: N = 15(135). Layer D: N = 15(109). FWHM denotes the full width at half maximum value. 95% confidence intervals are denoted in parentheses. For speed tuning measurements used to build the tuning width prediction in **(G)**, Layer A: N = 3–14(11–108); Layer B: N = 3–15(17–106); Layer C: N = 4–15(25–135), and Layer D: N = 4–15(20–109). See also Figure S7.

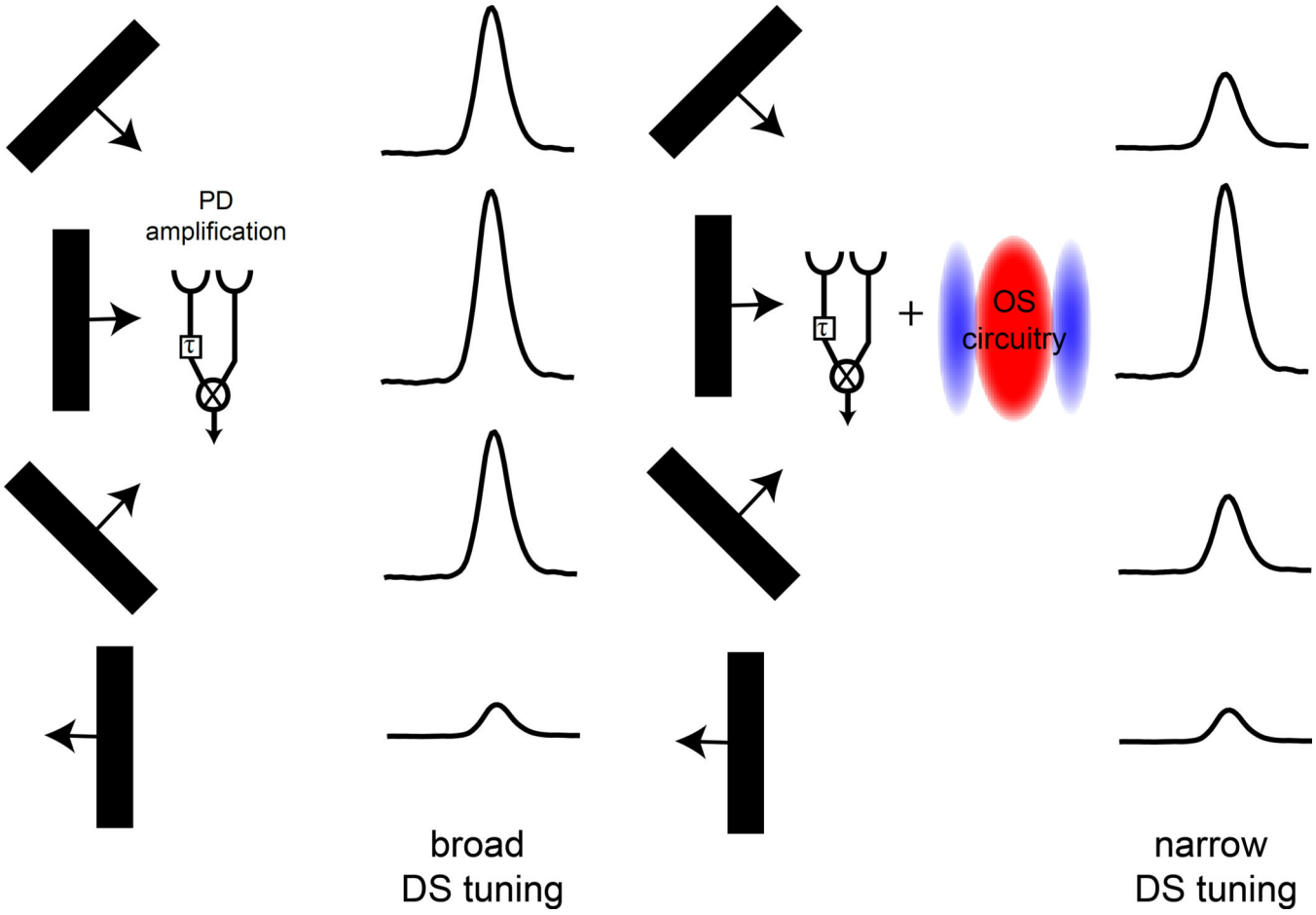

Figure 8. An interaction between OS and DS sharpens DS tuning

A schematic summarizing how OS and DS properties of T4 and T5 can combine to narrow directional tuning. A HRC model demonstrates how preferred direction amplification leads to broad directional responses. This tuning can be made narrower by adding OS circuitry that suppresses responses to stimuli that are oriented slightly off axis.